Extending a turbid medium BRDF model to allow sloping terrain with a vertical plant stand

Bruno Combal, Harumi Isaka, Craig Trotter

Extending a Turbid Medium BRDF Model to Allow Sloping Terrain with a Vertical Plant Stand

Bruno Combal, Harumi Isaka, and Craig Trotter

***Abstract*—This paper extends the turbid medium approach used for modeling bidirectional reflectance from horizontal plant canopies to sloping terrain with a vertically oriented plant stand. Previous treatments have accounted for terrain slope by simple adaptation to an inclined plane of models for horizontal surfaces. However, such treatments implicitly assume that plants grow perpendicularly to the surface, despite the fact that plant stems continue to grow vertically on slopes. We investigate the differences between our new "vertical growth" model and the more usual "perpendicular to the surface growth" model in terms of the effect on canopy albedo and bidirectional reflectance factors. Although the effect of leaf angle distribution on the albedo is different for both the vertical-growth and perpendicular-growth models, it appears to be a much smaller effect than that due to terrain slope. For the bidirectional reflectance factors (BRF's), the magnitude and sign of the differences between the two models varies with the direction of observation, the slope, and the leaf angle distribution, and can exceed 10% for a planophile canopy. A comparison between modeled and measured data shows that model predictions under the vertical growth assumption are consistent with measurements, whereas the assumption of perpendicular growth can lead to large errors.**

***Index Terms*—Albedo, BRF, slope, vertical plant stand.**

I. Introduction

THE modeling of bidirectional reflectance factors (BRF's) of a vegetation canopy is a crucial element for remote sensing of physical, biophysical, and canopy architectural characteristics of the land surface at global and regional scales. The retrieval of these characteristics from satellite observations must be based on an appropriate BRF model. Many measurements have revealed a pronounced anisotropy of the radiation field reflected from natural vegetation. The BRF model has not only to take into account all the physical, biophysical, and morphological characteristics of the vegetation canopy, but also the topography of the terrain on which the plants grow [1]–[3]. The choice of a suitable BRF model is a compromise between good agreement with experimental observations and reasonable computational cost. Accordingly, one-dimensional (1-D) BRF models [4]–[6] are often chosen from among the many models currently available for the retrieval of vegetation properties.

The usual way to remove the effect of topography from satellite data (in particular from Landsat TM images), consists of transforming the tilted surface to a horizontal one by modifying the upper boundary condition [7]. Frequently used methods are the Lambert cosine correction [8] and the Minnaert correction [9]. However, these types of corrections aim only at image normalization. Many attempts have also been made to correct for the effect of topography on the BRF by using 1-D models of vegetation canopies [8], [10]–[12]. To date, use of these models has involved the implicit assumption that plant growth is perpendicular to the ground surface. We hereafter refer to this type of model as the Perpendicular to the Ground Vegetation Model (PGVM). However, it is readily apparent that, with few exceptions, trees tend to grow vertically whatever the terrain slope. This means that we have to consider two additional effects on the anisotropy of the radiation field when vegetation is on a slope, compared with when it is on a horizontal surface and compared to the effect of terrain slope and the effect of the vertical orientation of plant stands.

The purpose of the present paper is to investigate the effect of integrating terrain slope and vertical plant growth into BRF's using the framework of a 1-D vegetation canopy model. Such a model enables the contribution of the terrain slope and plant stand orientation to BRF anisotropy to be examined separately, as a function of the type of leaf orientation. Hereafter, we refer to this type of model as the Vertical Vegetation Model (VVM).

The VVM presented below is basically an adaptation of the turbid medium model proposed by Ross [13]. We consider directly the effect of the terrain slope on the architectural characteristics of the plants and accordingly modify the radiative properties of the canopy. The hot spot effect is modeled according to Verstraete [4], but we take into account the effect of terrain slope on the hot spot geometry. We investigate the differences between the VVM and PGVM assumptions by comparing albedos and BRF's calculated using the two models, for a variety of canopy leaf angle distributions. Results from the models are also compared with some recent experimental measurements.

II. Radiation Transport in a Vegetation Canopy Growing on Tilted Terrain

A. Radiative Transfer Equation

The plant canopy on a tilted terrain is represented as a layer bounded by two parallel planes, a flat lower canopy surface and a flat canopy top surface, both of which are parallel to the ground

Manuscript received Sept. 24, 1998; revised April 16, 1999. The theoretical part of the investigation done by B. Combal and H. Isaka was conducted under joint grants from the Japanese National Space Development Agency (NASDA) under GLI/ADEOS-II Project G-0033 and the French National Institute for Sciences of the Universe (INSU) under Grant 96/ATP/494/220.2. Experimental investigations by C. Trotter were funded jointly by NASDA GLI/ADEOS-II Project G-0019 and the New Zealand Foundation for Research, Science, and Technology Contract C09620.

B. Combal and H. Isaka are with the Laboratoire de Météorologie Physique (LaMP), UPRESA 6016, Université Blaise Pascal, Clermont-Ferrand, France.

C. Trotter is with Landcare Research, Palmerston North, New Zealand.

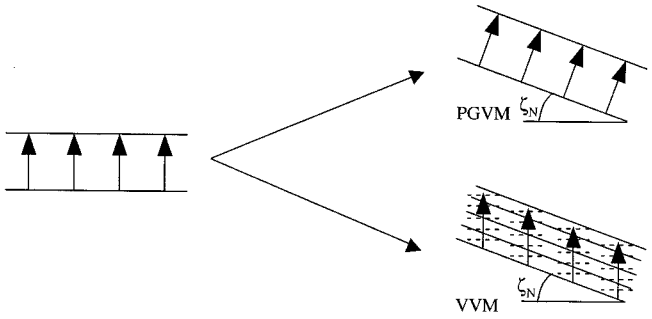

Fig. 1. Two approaches to correcting for the effects of slope by modifying the upper limit condition (sun position). In the widely-applied PGVM approach, the vegetation is implicitly assumed to grow perpendicularly to the slope. The VVM approach assumes the vegetation remains vertical as the terrain is tilted.

surface. To compute the radiative transfer within and from the vegetation canopy, we consider the canopy top to be illuminated by monodirectional incident light. The effect of diffuse sky irradiance, path irradiance, and diffuse irradiance from surrounding terrain, is neglected. In this case, we can compute the radiation field from the canopy on the tilted terrain by modifying only the condition of direct illumination. Fig. 1 represents schematically a vegetation canopy growing on tilted terrain for both the PGVM and VVM models.

The canopy layer is assumed to be uniformly filled with scattering and absorbing leaves. Radiation of intensity I propagating through a cylinder with length ∂r and unit cross–section oriented at right angles to the direction $\underline{\Omega}'$ is decreased by scattering and absorption and increased by intensities scattered from the direction $\underline{\Omega}$ into the direction $\underline{\Omega}$. The radiation balance in this homogeneous cylinder is [14]

$$\partial I = -\sigma(\underline{\Omega})\partial r\ I(\underline{\Omega}) + \left(\int_{4\pi} \sigma_s(\underline{\Omega}' \rightarrow \underline{\Omega}) I(\underline{\Omega})\ d\underline{\Omega}'\right)\partial r \tag{1}$$

where $\sigma(\underline{\Omega})$ is the volume cross-section of photon interaction along the direction $\underline{\Omega}$, and $\sigma_s(\underline{\Omega}' \rightarrow \underline{\Omega})$ is the differential cross-section in the same direction for intensities coming from direction $\underline{\Omega}'$. To deal with the radiative transfer through the plant canopy on tilted ground, we need to define two coordinate systems, S_1 and S_2 (Fig. 2). The S_1 coordinate system is defined by the unit vectors $\underline{u}$ and $\underline{v}$ in the horizontal plane and by the vertical unit vector $\underline{w}$. The S_2 coordinate system is a local system associated with the tilted canopy surface and is defined by the three unit vectors $\underline{J}$, $\underline{J'}$, and $\underline{N}$. The unit vector $\underline{J}$ is taken along the direction of the steepest slope in the tilted plane, the unit vector $\underline{J'} = \underline{N} \times \underline{J}$ is perpendicular to $\underline{J}$ and parallel to the ground, and the unit vector $\underline{N}$ is normal to the tilted terrain. In the S_1 system, these unit vectors are expressed as $\underline{J}(\zeta_J, \eta_J)$, $\underline{J'}(\zeta_{J'}, \eta_{J'})$, and $\underline{N}(\zeta_N, \eta_N)$, where the angles ζ and η designate the zenith and azimuth angles, respectively, of the tilted terrain in the S_1 system. The components $(\Omega_u, \Omega_v, \Omega_w)$ of the direction vector $\underline{\Omega}$ in the S_1 system are transformed into $(\Omega_J, \Omega_{J'}, \Omega_N)$ in the S_2 coordinate system with a rotational matrix P defined with respect to the $\underline{J}$, $\underline{J'}$, and $\underline{N}$ system

$$(\Omega_J, \Omega_{J'}, \Omega_N) = P(\Omega_u, \Omega_v, \Omega_w). \tag{2}$$

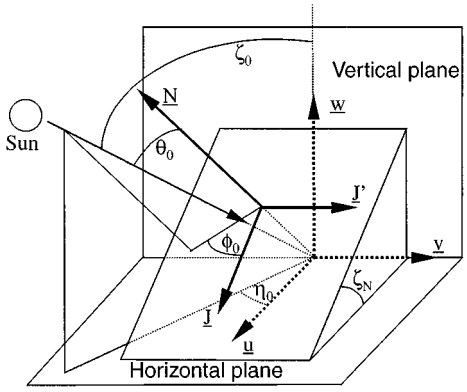

Fig. 2. Coordinate system S_1 is independent of the slope, and S_2 is related to the sloping terrain.

The 1-D hypothesis requires that the canopy be modeled as a stratified medium with parallel homogeneous planar layers. Vegetation growing vertically can be regarded as axisymmetric and can be arranged in horizontal layers. When the vegetation is growing on sloped terrain, the axis of the slope normal and the axis of symmetry of the plants does not, in general, coincide. Thus, we invoke the simplifying assumption of a uniform vegetation cover where all the layers are filled in an identical manner.

Let us consider a vertical coordinate z linked to the elementary cylinder ∂r

$$\partial r = \frac{\partial z}{\mu} \tag{3}$$

where $\mu = \cos\theta$, and θ is the zenith angle of the propagating direction $\underline{\Omega}$ with respect to the unit vector $\underline{N}$. Since we assume uniform canopy properties, we can write (1) as

$$\mu\frac{\partial I(z,\underline{\Omega})}{\partial z} = -\sigma(\underline{\Omega})I(z,\underline{\Omega}) + \int_{4\pi} \sigma_s(\underline{\Omega}' \rightarrow \underline{\Omega})I(z,\underline{\Omega})\ d\underline{\Omega}' \tag{4}$$

where z is measured in a positive upwards direction along the vector $\underline{N}$. The direction $\underline{\Omega}(\theta, \phi)$ is given by the zenith angle θ and the azimuth angle ϕ with respect to orientation of the canopy surface in the S_2 coordinate system.

The upper boundary condition at $z = z_t$ is given by the monodirectional source with an intensity π and an incident direction $\underline{\Omega}_0(\theta_0, \phi_0) \in [-2\pi, 0]$ in the S_2 coordinate system

$$\begin{aligned} &I(z,\underline{\Omega}) = \pi\delta(\underline{\Omega} - \underline{\Omega}_0) \qquad \mu < 0, \mu' < 0 \\ &\underline{N} \cdot \underline{\Omega}_0 < 0. \end{aligned} \tag{5}$$

The incident light is seen from the ground only for the condition $\underline{N} \cdot \underline{\Omega}_0 < 0$. The lower boundary condition at $z = 0$ is given by

$$\begin{aligned} I(0,\Omega) = \frac{R_s}{\pi} \int_{2\pi^-} |\mu'| I(0,\underline{\Omega}')\ d\underline{\Omega}' \\ \mu > 0, \mu' < 0. \end{aligned} \tag{6}$$

where $2\pi^-$ is the set of downwards direction (i.e., $\mu' < 0$ and $\phi \in [0, 2\pi]$). The solution I of the radiative transfer equation is separated into three terms: nonscattered radiation (I^0),

singly scattered radiation (I^1), and multiple scattering (I^M). An analytical formulation is used to calculate I^0 and I^1 [15]. The multiple scattering is computed with the Discrete Ordinate Method (DOM) algorithm for a 1-D, two-angles geometry [16], but without any symmetry for the phase function, since the vegetation vertical axis and the axis used for computation (i.e., $\underline{N}$) do not coincide. The computed radiation field is that for the S_2 coordinate system. Evaluation of the radiative transfer equation (4), according to the boundary conditions (5) and (6), is sufficient to formulate the PGVM model. However, formulation of the VVM requires that the vegetation properties $\sigma(\underline{\Omega})$ and $\sigma_s(\underline{\Omega}' \rightarrow \underline{\Omega})$ be modified. The following section describes this modification.

B. Optical Properties of the Tilted Canopy

In the vegetation layer, only the leaves are considered. The medium is thus approximated by a turbid medium [13], [16], to which is added a function to describe the hot spot in order to account for the shadow-hiding phenomenon [4], [17]. The properties of the medium thus rely on just two factors: the typical turbid medium characteristics (attenuation and scattering) and the hot spot function.

1) Leaf Angle Distribution (LAD): A uniform horizontal canopy can be characterized by an LAD. The LAD is denoted by the function $g_L(\underline{\Omega}_L)$ and can be approximated by a variety of analytical forms [13], [18]. The most widely used LAD models are Bunnik's discrete LAD [19], the elliptical distribution [5], and the beta distribution [20]. In this paper, we use Bunnik's distribution, which consists of five discrete and typical classes: planophile (mostly horizontal leaves), erectophile (mostly vertical leaves), plagiophile (most of the leaves at 45°), and extremophile (a combination of "melting" planophile and erectophile), and uniform.

When plants grow vertically on tilted terrain, the LAD can still be defined by $g_L(\underline{\Omega}_L)$ in the S_1 coordinate space. However, we have to represent it in S_2 coordinate space to calculate the radiant intensity $I(z, \underline{\Omega})$ reflected by the vegetation. We express hereafter the direction $\underline{\Omega}$ as either $\underline{\Omega}_1$ or $\underline{\Omega}_2$ to make explicit the coordinate system in which the direction is being considered. To calculate the intensity in direction $\underline{\Omega}_2$, we need to know the vegetation properties in the direction $\underline{\Omega}_2$ in S_2 coordinates at a given value of z. These properties are given by the $g_L(\underline{\Omega}_L)$ function in S_1 coordinate space, in the direction $\underline{\Omega}_1 = P^{-1}\underline{\Omega}_2$. The distribution function $g_L(\underline{\Omega}_L)$ is assumed to be the product of two independent distribution functions that depend on the zenith angle ζ and azimuth angle η of the leaf normals in the S_1 system. Moreover, the azimuthal distribution of the leaf normals may be assumed to be random (i.e., the vegetation is considered to be axisymmetric about the vertical axis. Hence, the LAD can be fully represented by the distribution function of leaf zenith angle $g_L(\zeta_L)$ only. However, we need two angles to represent the LAD of a uniform canopy on tilted ground in S_2 coordinates, because the axis of canopy symmetry and the normal and the ground no longer coincide (Fig. 2). Hence, for the VVM, the total interaction cross-section and the differential scattering cross-sections of the leaves change with the geometrical relationship between the ground slope and incident radiation.

2) Optical Properties of a Turbid Medium: Following [13], the attenuation and scattering processes are represented respectively by $G(\underline{\Omega})$ and $\Gamma(\underline{\Omega}' \rightarrow \underline{\Omega}, \underline{\Omega}_L)$, where $\underline{\Omega}_L$ is the leaf orientation. As done for the $g_L(\underline{\Omega}_L)$ function, we only need to transform the direction $\underline{\Omega}_2$ to the direction $\underline{\Omega}_1$ to take into account of the effect of ground slope on $G(\underline{\Omega})$ and $\Gamma(\underline{\Omega}' \rightarrow \underline{\Omega}, \underline{\Omega}_L)$, which are again defined first in S_1 coordinates

$$\begin{aligned} G_2(\underline{\Omega}_2) &= G_1(P^{-1}\underline{\Omega}_2) \\ \Gamma_2(\underline{\Omega}'_2 \rightarrow \underline{\Omega}_2, \underline{\Omega}_{L2}) &= \Gamma_1(P^{-1}\underline{\Omega}'_1 \rightarrow P^{-1}\underline{\Omega}_1, P^{-1}\underline{\Omega}_{L1}). \end{aligned} \tag{7}$$

The function $G(\underline{\Omega})$ represents the total interaction cross-section of leaves per unit volume in the direction $\underline{\Omega}$ [13], [21]

$$G(\underline{\Omega}) = \int_{2\pi^+} \frac{g_L(\underline{\Omega}_L)}{2\pi} |\vec{\underline{\Omega}}_L \cdot \underline{\Omega}| \, d\underline{\Omega}_L \tag{8}$$

The term $(1/2\pi)[g_L(\underline{\Omega}_L)|\underline{\Omega}_L \cdot \underline{\Omega}|] \, d\underline{\Omega}_L$ is the projected area of leaves that have normals within the solid angle $d\underline{\Omega}_L$ around the direction $\underline{\Omega}_L$, onto a plane perpendicular to the direction $\underline{\Omega}$. For a homogeneous vegetation medium with a constant leaf density u_L, the leaf area index (LAI) can be expressed as

$$L(z, \underline{\Omega}) = G(\underline{\Omega}) u_L \frac{z}{\mu}. \tag{9}$$

The scattering of light from the direction $\underline{\Omega}'_2$ into the direction $\underline{\Omega}_2$ is defined for an axisymmetric LAD as [18]

$$\begin{aligned} &\frac{1}{\pi}\Gamma(\underline{\Omega}' \rightarrow \underline{\Omega}) \\ &\quad = \frac{1}{2\pi} \int_{2\pi} g_L(\underline{\Omega}_L) |\underline{\Omega}' \cdot \underline{\Omega}_L| f(\underline{\Omega}' \rightarrow \underline{\Omega}, \underline{\Omega}_L) \, d\underline{\Omega}_L \end{aligned} \tag{10}$$

where the function $f(\underline{\Omega}' \rightarrow \underline{\Omega})$ models the scattering scheme of an individual leaf, assumed to be bi-Lambertian [18]

$$f(\underline{\Omega}' \rightarrow \underline{\Omega}) = \begin{cases} r_l |\underline{\Omega} \cdot \underline{\Omega}_L|/\pi, & (\underline{\Omega} \cdot \underline{\Omega}_L)(\underline{\Omega}' \cdot \underline{\Omega}_L) < 0 \\ t_l |\underline{\Omega} \cdot \underline{\Omega}_L|/\pi, & (\underline{\Omega} \cdot \underline{\Omega}_L)(\underline{\Omega}' \cdot \underline{\Omega}_L) > 0 \end{cases} \tag{11}$$

For a plant stand growing vertically on a slope, we admit the same hypothesis and simplifications as for the LAD function in the S_1 coordinate system. Since the plant axis of symmetry does not coincide with the unit vector $\underline{N}$, (8) and (10) cannot be simplified as an integral over one angle in the S_2 system. Consequently, at each step of the calculation of (8) and (10), the function $g_L(\underline{\Omega}_L)$ has to be evaluated according to (2), where $\underline{\Omega}_L$ depends only on the zenith angle ζ in the S_1 system.

3) Hot Spot Correction: A range of models is available to describe the hot spot effect for a horizontal vegetation canopy. We have to adapt a hot spot model to the context of the VVM by taking into account the effect of terrain slope on the optical path length and leaf cross section with respect to an incident ray of light. Although the most widely used model of the hot spot is that of Kuusk (described in [22]), the formulation of Verstraete and colleagues [4] was chosen because it relies on geometrical considerations which can be easily adapted to the VVM situation.

In real plant canopies, the leaves are discrete scatterers separated from each other by gaps. If an incident ray of light passes

TABLE I
OPTICAL PROPERTIES OF LEAVES AND SOIL

	Leaf reflectance	Leaf transmittance	Soil albedo
RED	0.075	0.05	0.03
NIR	0.5	0.45	0.15

TABLE II
COMMON CONDITIONS FOR THE SIMULATIONS

Parameters	Values
Sun position	$\zeta_0 = 32°$, $\eta_0 = 0°$
Hot spot	$r_{sf} = 0.1$ m
Layer thickness	$z_t = 1, 2, 5, 10$ m

through a gap down to a given depth in the vegetation canopy, where it encounters a leaf, it will be scattered back in the sun direction unattenuated [23] except for the energy absorbed by the leaf. However, for scattering directions significantly different from the sun direction, the attenuation of the scattered radiation is determined by $\sigma(\underline{\Omega})$, the coefficient of extinction of the canopy. When the terrain is tilted, $\sigma(\underline{\Omega})$ must be corrected to take account of the modification of the optical path compared with that in a horizontal canopy. In a horizontal canopy, a cylindrical sun beam penetrating down into the vegetation has a radius r_{sf} equal to the interstitial interval (in a statistical sense) between the leaves. The correction applied to the coefficient of extinction is thus parameterized by r_{sf} [4]. If the terrain is tilted the vegetation remains vertical, as does the space between leaves. Since the calculations are made with respect to the terrain normal, the circular cross-section of the incoming beam is seen in the S_2 coordinate system as an elliptical cross-section. Accordingly, we define for the S_2 system a circular cross-section of equivalent area to the ellipse, with a radius $\tilde{r}$ given by

$$\tilde{r} = r_{sf}\sqrt{\frac{|\underline{\Omega}_0 \cdot \underline{w}|}{|\underline{\Omega}_0 \cdot \underline{N}|}} \tag{12}$$

The equivalent circular cross-section with radius $\tilde{r}$ represents the hot spot parameter appropriate for vegetation growing vertically on a slope. For the particular case of horizontal terrain, we have $\tilde{r} = r_{sf}$.

III. EVALUATION OF THE PLANT STAND ORIENTATION EFFECT

Two factors have to be considered when modeling the effect of topography on radiation reflected by vegetation canopies. The first factor is the terrain slope itself, and the second is the tendency of plant stands to remain oriented vertically regardless of slope. In this section, we show how the orientation of the plant stand affects both the albedo and BRF of vegetation canopies, by comparing results from simulations using the VVM and PGVM. This is investigated as a function of vegetation type as represented by variations in the LAD. Predictions from the VVM and PGVM are also compared with measurements of reflectance obtained for a vegetation canopy on a relatively steep slope.

A. Conditions of the Simulations

The reflectance and transmittance of the bi-Lambertian leaves and the soil albedo we used are reported in Table I and correspond to typical values of vegetation optical properties observed at red and near-infrared (NIR) wavelengths [24]. Table II lists the conditions common to all simulations. The soil was chosen as dark because we are primarily interested in the effect of vegetation properties on the albedo and BRF. To compute the radiation field for various values of the LAI, we fixed the leaf density u_L constant equal to 1 m^2m^{-3} and varied the depth of the vegetation canopy z_t from 1 m to 10 m. Thus, increases in z_t simulates an increasing LAI, and z_t should be understood as an optical depth and not as a real length. Note that a given value of leaf density for a horizontal canopy will result in differing values of LAI under the differing plant stand orientation assumptions in the VVM and PGVM for nonrandom LAD's.

In the present study, we used a constant sun zenith angle of 32° with respect to the S_1 coordinate system. We tilted the terrain in such a way that the principal plane was always kept perpendicular to the tilted terrain. With this configuration, the sun incidence angle with respect to the terrain may assume values over the entire possible range. When the normal to the terrain has an azimuth η_N = 0°, the terrain is tilted in the direction of the sun, and when the normal has an azimuth of η_N = 180°, the terrain is tilted in the direction opposite the sun. To allow a comparison with experimental data only, simulations were also performed for the slope oriented at η_N = 90° (Section II-D).

B. Impact of Plant Stand Orientation on the Albedo and BRF

The difference between the VVM and PGVM approaches resides only in the differing assumptions that the two models make about plant stand orientation. We now examine the variation in the values of albedo and BRF calculated using the two models as a function of terrain slope angle. The sloped terrain is illuminated by the sun only if the condition in (5) is satisfied. In all calculations and graphics that follow, the values of albedo and BRF are derived from the radiant energy that upwells from the surface through a horizontal plane (that is, the values are reported with respect to coordinate system S_1).

1) The Albedo: Fig. 3 represents the albedo at red wavelengths for a vegetation canopy with an optical depth of 1 m as a function of terrain slope for Bunnik's five LAD's. For data presented in this figure, we have not considered the hot spot effect.

The values of albedo calculated from both the VVM and PGVM exhibit quite similar variations with terrain slope. For both models, the albedo is always larger for a tilted surface than for a horizontal surface whenever the terrain is tilted toward the sun with a slope angle less than about 50°. For example, the PGVM albedo for planophile leaves is about 0.029 for a horizontal surface, while it increases to the maximal value of 0.033 (an increase of more than 10%) for terrain tilted by 20°. The maximal albedo occurs, for most of the plant types, when the terrain is tilted toward the sun direction by an angle of about 20°. This means that the maximal energy is reflected from the sloped terrain when the incident radiation is not exactly normal to the terrain. The albedo of the tilted surface becomes smaller than the albedo of the horizontal surface only when the terrain is tilted away from the sun direction or when tilted toward the sun

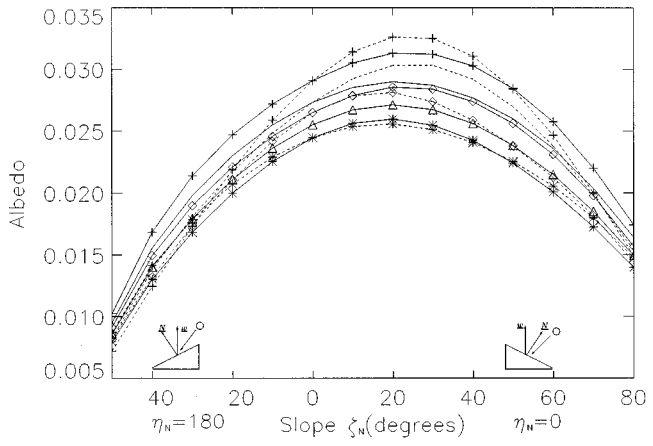

Fig. 3. Albedos computed with the PGVM (dotted lines) and VVM (continuous lines) with respect to the terrain slope for red wavelengths $z_t = 1$ m and no hot spot. The LAD's are: +: planophile, $*$: erectophile, –: plagiophile, $\diamond$: extremophile, and $\triangle$: uniform. Slope angles to the right of zero are tilted toward the sun ($\eta_N = 0°$), whereas those to the left of zero are tilted away from the sun ($\eta_N = 180°$).

direction by a very large angle. That is, whenever the incidence angle for the tilted surface is larger than that for the horizontal surface.

Fig. 3 shows that the albedo varies with the preferred orientation of leaves. The variation decreases in the order of planophile, plagiophile, extremophile, uniform, and erectophile for any terrain slope, for both the PGVM and VVM. This variation of the albedo with LAD is expected, because regardless of the plant stand orientation adopted in the models, the total interaction cross-section of leaves increases with sun irradiance as the leaf orientation becomes more horizontal. In spite of this similar behavior overall, there are some interesting differences between the albedos predicted by the VVM and PGVM. As the incidence angle with respect to the tilted terrain surface becomes large, the albedo of the tilted surface calculated using the PGVM becomes quasi-independent of the leaf orientation (the effect due to LAD tends to disappear). In contrast, the LAD has a significant effect on albedos calculated with the VVM at all incidence angles. These trends are expected, because the sun-leaf orientation geometry does not change with terrain slope in the VVM as it does in the PGVM.

In order to make the plant stand orientation effect more clear, we computed a relative difference $\rho(\zeta_N)$ for the albedos calculated from the VVM and PGVM. It is defined as

$$\rho(\zeta_N) = \frac{A(\zeta_N)_{VVM} - A(\zeta_N)_{PGVM}}{A(\zeta_N)_{VVM}} \qquad (13)$$

where $A(\zeta_N)$ is the albedo of a vegetation canopy with a slope of ζ_N, and the subscripts 'VVM' and 'PGVM' stand for the VVM and the PGVM approaches, respectively.

Fig. 4 (red wavelengths) and Fig. 5 (NIR wavelengths) show the relative difference in albedo as a function of terrain slope and LAD. In Fig. 4, the upper figures are for an optical depth of 1 m, and the lower figures are for an optical depth of 10 m. To provide data for these graphics, we computed the albedo according to the VVM and PGVM with and without the hot spot correction. The graphics without the hot spot correction are given on the left, and those with the hot spot correction are on the right. As expected, there is no difference in the albedo between the VVM and PGVM for the uniform LAD when the hot spot correction is not considered. A slight difference of less than 1% can be observed when this correction is included, due to the small differences between the hot spot radius for the two models. Because it has little effect on the albedo, in Fig. 5, the hot spot is not considered. For LAD's other than uniform, in Figs. 4 and 5, the variation of the albedo relative difference with terrain slope changes significantly with leaf orientatio (in other words, with the type of vegetation). Note that the albedo calculated from the VVM is the same as that from the PGVM for the case of horizontal terrain $\zeta_N = 0°$ for all the LAD's, as expected.

Since the overall variation in the albedo relative difference is quite similar for all the figures in Figs. 4 and 5, the comments that follow in this paragraph are made using the results for the 1-m optical depth canopy as a typical example [Fig. 4(a)]. For the planophile LAD, as the terrain slope varies from 50° away from the sun direction to 20° toward it, the relative difference $\rho(\zeta_N)$ at red wavelengths decreases from +0.3 to a minimum of about –0.04. Then, as the slope of the terrain increases from 20° toward the sun to 80° toward the sun, it increases from the minimum to about +0.14. The plagiophile LAD exhibits a similar variation, except it decreases from about +0.13 to about –0.05, then increases to +0.08. The minimum relative difference occurs for slopes of about 30° to 40° toward the sun for the plagiophile LAD. For the erectophile LAD, we observe a reverse variation. As the terrain slope varies from 50° away from the sun to 20° toward the sun, the relative difference $\rho(\zeta_N)$ at red wavelengths increases from –0.10 to a maximum of about +0.02. Then, as the slope of the terrain continues to increase from 20° toward the sun to 80° toward the sun, the relative difference decreases from the maximum to about –0.06. For the extremophile LAD, which is a mixture of the planophile and erectophile, the albedo relative difference varies like the planophile LAD, except that it does not exhibit any negative value, and it tends to saturate at about +0.08 beyond a slope angle of about 60°. This behavior can be interpreted as resulting from the compensation of two opposing trends in the variation of the relative difference of the planophile and erectophile LAD's. Note that this compensation happens in spite of the fact that the planophile LAD shows an albedo relative difference with a negative excursion that is greater in magnitude than the positive excursion for the erectophile LAD.

When the optical depth of the canopy increases from 1 m to 10 m, the variation of $\rho(\zeta_N)$ with terrain slope exhibits only a very slight increase at red wavelengths, and a slight shift of the slope angle corresponding to the minimum or maximum relative difference for each LAD. This may be due to the large absorption of red light by leaves. For NIR wavelengths (Fig. 5), the situation is quite different. The increase in the optical depth (and consequently the LAI) of the canopy by a factor of ten results in a reduction of the relative difference by about 50% for positive excursions of the relative difference for the planophile and plagiophile LAD's, and for the negative excursion of the erectophile LAD. However, it is interesting that such a large reduction is not seen for negative excursions of the relative difference

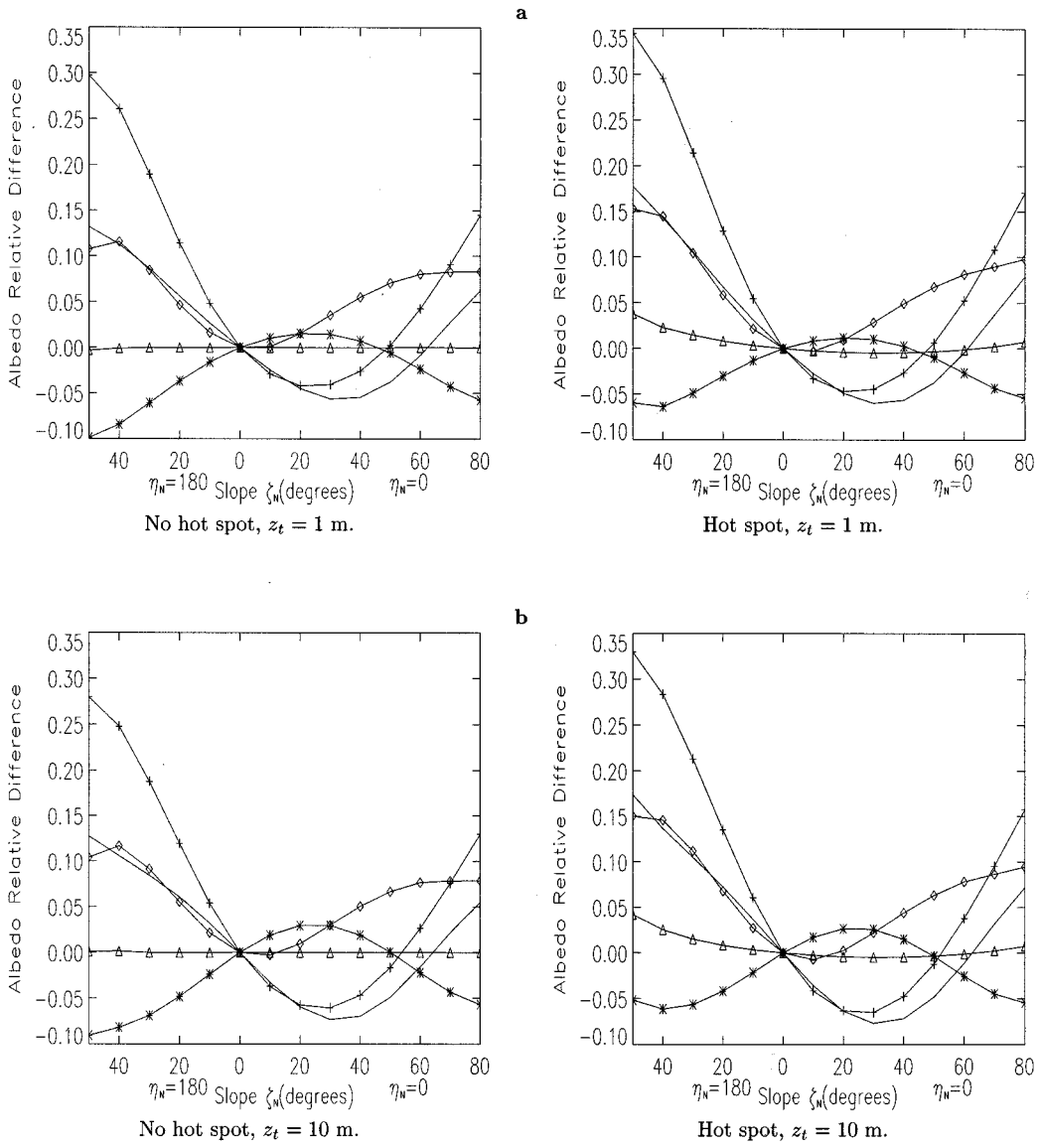

Fig. 4. Comparison of albedos for red wavelengths. Figures on left: no hot spot. Figures on the right: $r_{sf} = 0.1$ m. Figures at the top (a): $z_t = 1$ m. Figures at the bottom (b): $z_t = 10$ m. The LAD's are +: planophile, $*$: erectophile, −: plagiophile, $\diamond$: extremophile, and $\triangle$: uniform. Slope angles to the right of zero are tilted toward the sun ($\eta_N = 0°$), whereas those to the left of zero are tilted away from the sun ($\eta_N = 180°$).

for the planophile and plagiophile LAD's, nor for the positive excursion of the erectophile LAD.

The above results show that the effect of plant stand orientation on the albedo varies with the type of vegetation, the wavelength, and the canopy LAI. However, it is also apparent that plant stand orientation affects the albedo to a much smaller extent than does terrain slope by itself. These results are not completely unexpected, because the albedo is an integral parameter that tends to smooth out local differences in bidirectional reflectance.

2) The BRF: To evaluate the effect of terrain slope and plant stand orientation on the BRF, we computed the BRF for the VVM and PGVM with the hot spot correction included. We considered the two cases of the principal plane set perpendicular to the tilted terrain, with the terrain normal in the direction (ζ_N =20°, $\eta_N = 0°$ or 180°). The sun direction is given by $\zeta_0 = 32°$ and $\eta_0 = 0°$, and the hot spot parameter was taken as $r_{sf} =$ 0.1 m. To compare the BRF between the VVM and PGVM, we again calculate a relative difference, this time for the BRF as defined by

$$\rho(\zeta_N, \underline{\Omega}_V) = \frac{BRF(\zeta_N, \underline{\Omega}_V)_{VVM} - BRF(\zeta_N, \underline{\Omega}_V)_{PGVM}}{BRF(\zeta_N, \underline{\Omega}_V)_{VVM}} \quad (14)$$

where $BRF(\zeta_N, \underline{\Omega}_V)$ represents the bidirectional reflectance factor in the direction $\underline{\Omega}_V$ in the S_1 coordinate system. The directional distribution of the relative difference $\rho(\zeta_N, \underline{\Omega}_V)$ is plotted as three-dimensional (3-D) surface and two-dimensional (2-D) iso-contour graphics (Figs. 7 and 8). The center of the plots is the nadir direction in the S_1 system (Fig. 2). The concentric circles in the iso-contour plots indicate the view zenith

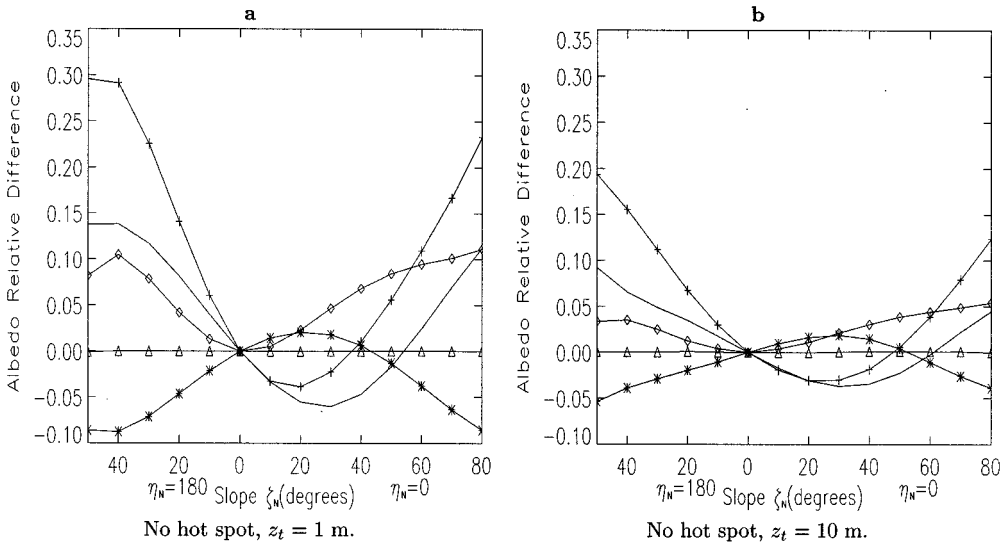

Fig. 5. Comparison of albedos for NIR wavelengths without the hot spot. Figure on the left (a): $z_t = 1$ m, figure on the right (b): $z_t = 10$ m. The LAD's are +: planophile, $*$: erectophile, −: plagiophile, $\diamondsuit$: extremophile, and $\triangle$: uniform. Slope angles to the right of zero are tilted toward the sun ($\eta_N = 0°$), whereas those to the left of zero are tilted away from the sun ($\eta_N = 180°$).

angle ζ_V every 10°. For tilted terrain, the radiation cannot be reflected upward from the tilted terrain into the complete upper hemisphere. Hence, the resulting $\rho(\zeta_N, \underline{\Omega}_V)$ plots lack some portion of the hemisphere depending on the direction of the terrain slope.

Let us consider first the uniform LAD, whose scattering phase function is isotropic. Consequently, its BRF without the hot spot correction should not depend on the terrain slope. However, when the hot spot correction is included, there is a very small difference in the BRF between the VVM and PGVM (Fig. 6). This occurs because the circular shape for the hot spot representation has a different cross-section for incident solar radiation depending on whether the vegetation is vertical or not. Fig. 6(a) corresponds to the BRF relative difference obtained for terrain tilted away from the sun direction by 20°, and Fig. 6(b) for terrain tilted toward the sun direction by 20°. For a slope tilted away from the sun, the hot spot correction leads to a modification of the BRF that results in a relative difference of about 2.5% near the hot spot direction. For directions away from the hot spot, the BRF relative difference remains at about 0.5% and does not depend on the observation direction Ω_V. For a slope tilted toward the sun direction ($\eta_N = 0°$), the interaction cross-section of the solar beam is larger for r_{sf} than for $\tilde{r}$, resulting in $BRF_{VVM} < BRF_{PGVM}$. This situation is inverted for a slope azimuth of η_N = 180°. In the exact hot spot direction, the BRF relative difference is zero since for isotropic scattering properties, the radiation entering from the sun direction and scattered back in this exact sun direction $\underline{\Omega}_0$ does not depend either on the hot spot radius or on the vegetation orientation direction. Only the radiation scattered in directions near the hot spot direction is significantly affected in different ways by the VVM and PGVM calculations. The relative difference between the PGVM and VVM is small, although not zero, in directions other than near the hot spot direction.

The relative differences of the BRF at red wavelengths are shown for the LAD's in Figs. 7 and 8 [(a) planophile, (b) erectophile, (c) plagiophile, and (d) extremophile]. Fig. 7 corresponds to tilting of the terrain by 20° toward the sun direction, and Fig. 8 to tilting of 20° away from it. The amplitude and sign of the relative difference for a given LAD vary greatly with the sun, viewing, and slope angle geometry. For the planophile LAD, Fig. 7 shows that the relative difference reaches about −25% for backward directions, while it becomes slightly positive (less than +5%) for forward directions. In contrast, Fig. 8(a) shows a similar directional distribution of the relative difference, but of the opposite sign: the relative difference reaches about +25% for backward directions, while it is slightly negative (less than −5%) for large forward directions. For the erectophile LAD [Figs. 7(b) and 8(b)], the BRF relative difference is always less than 5% in amplitude, while its sign is reversed from mainly positive [Fig. 7(b)] to mainly negative [Fig. 8(b)] as the slope tilts toward and away from the sun, respectively. For the plagiophile LAD, Fig. 7(c) exhibits a large region of slightly positive relative difference (less than +5%) around nadir and a narrow peripheral zone of large negative difference (more than −20%). In contrast, Fig. 8(c) shows the relative difference is negative (less than −5%) around the direction (ζ_V = 40°, η_V = 180°) and increases to +15% in the peripheral zone. For the extremophile LAD, the relative difference is small [negative in Fig. 7(d) and positive in Fig. 8(d)] in backward directions and increases to +20% [positive in Fig. 7(d) and negative in Fig. 8(d)] in forward directions.

These directional distributions of the BRF relative difference show that the plant stand orientation effect is more important for the planophile and extremophile LAD's than the plagiophile and erectophile LAD's, since horizontally oriented leaves intercept a larger amount of solar radiation than vertically oriented leaves. However, the plant stand orientation effect changes as a function of the incidence angle and azimuth

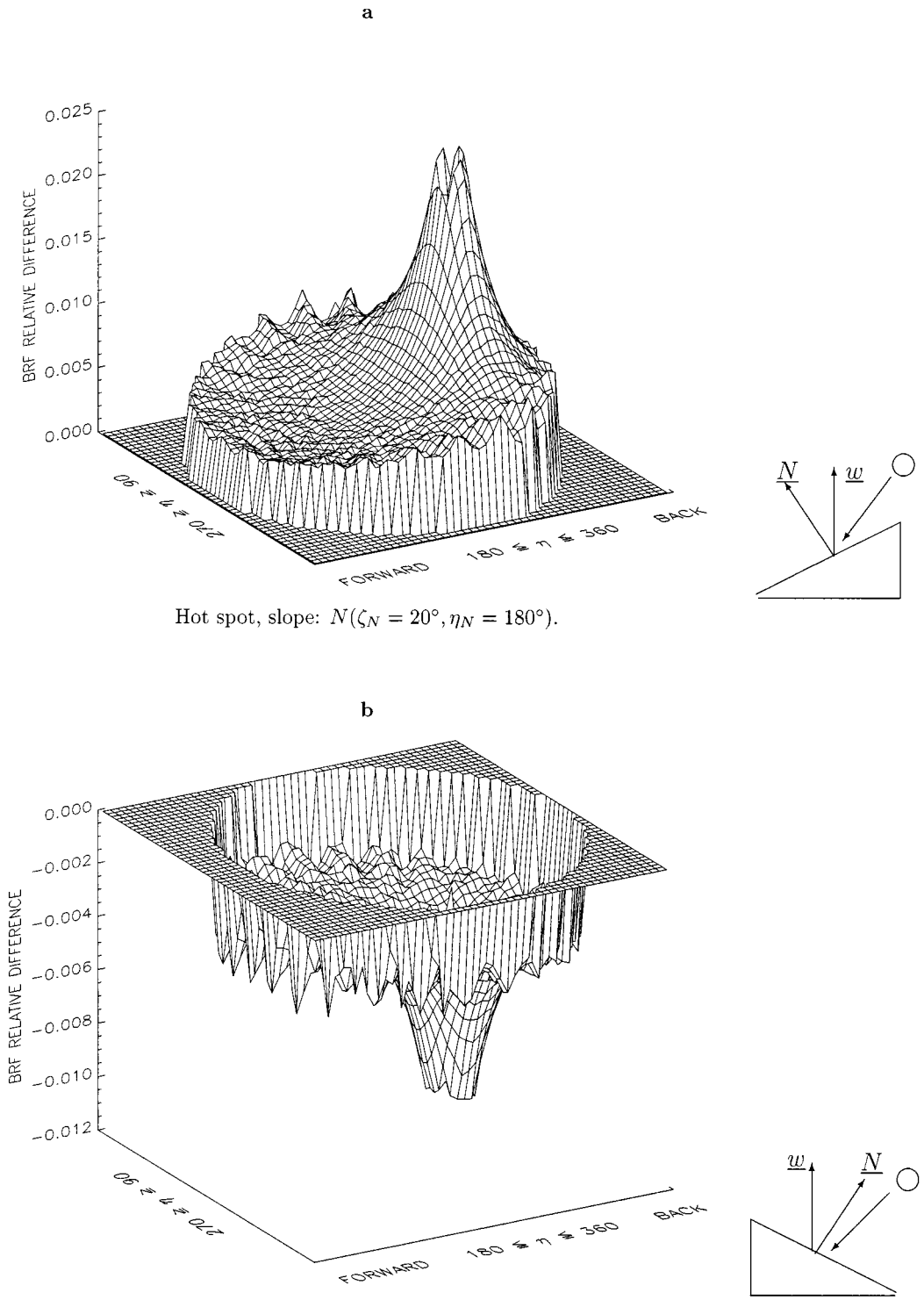

Fig. 6. Comparison of BRF's computed with the VVM and PGVM for a uniform LAD, with a hot spot ($r_{sf} = 0.1$ m), for red wavelengths.

angle of the radiation with respect to the tilted surface. The occurrence of positive and negative BRF relative differences for a given configuration explains why the albedo relative difference remains small for the plagiophile and extremophile LAD's.

3) Global Estimation of the Plant Stand Orientation Effect: Because the directional distribution of the BRF relative difference varies considerably from one configuration to another, it is rather difficult to provide an overall picture of its dependence on LAD and terrain orientation. The bidirectional reflectance distribution exhibits a complex shape with positive and negative regions, and often the BRF relative difference increases strongly for a large oblique viewing angle $\underline{\Omega}_V$. Hence, to provide a global picture of the plant stand orientation effect,

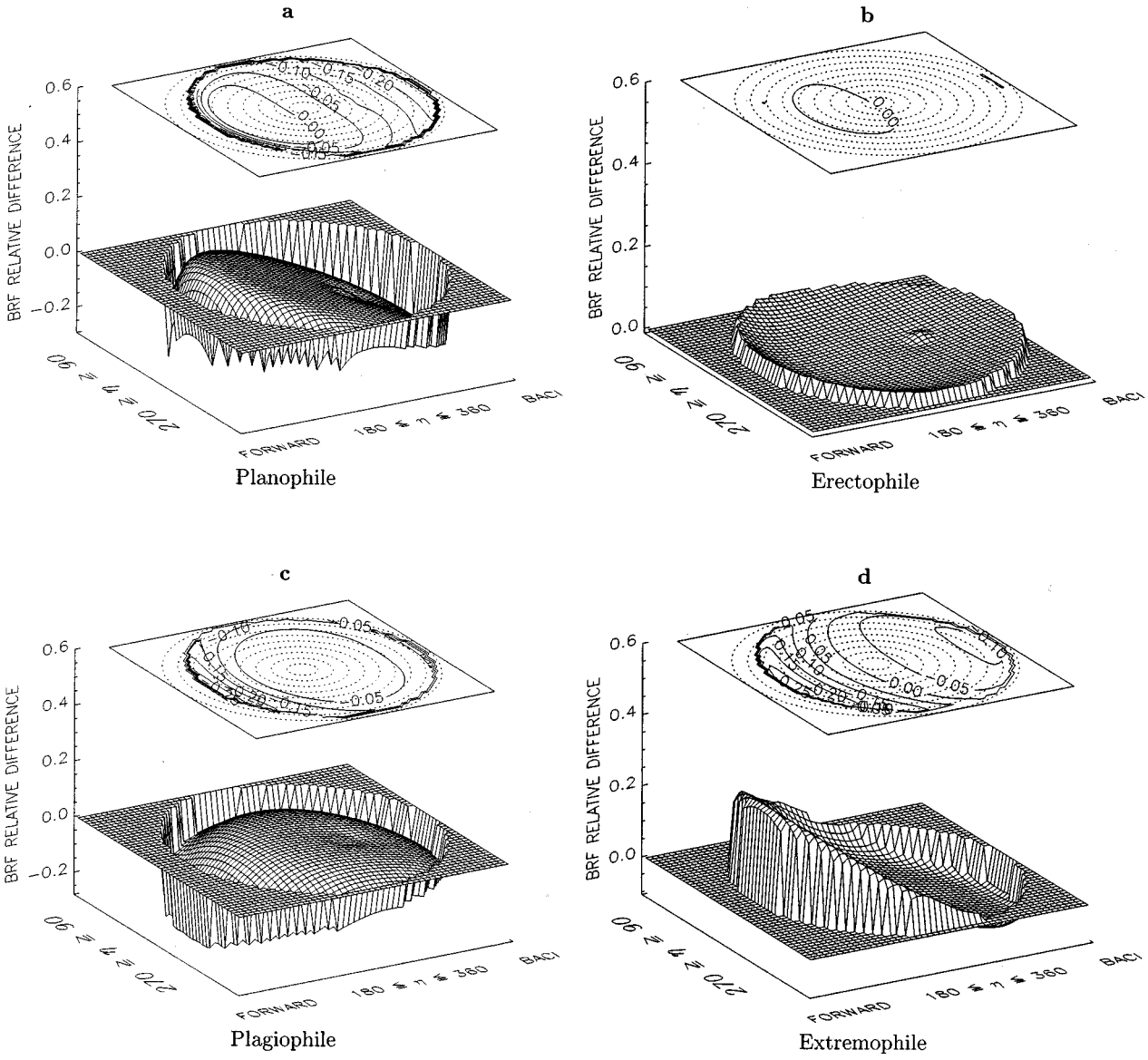

Fig. 7. BRF relative difference between the VVM and PGVM for red wavelengths. The terrain has a slope $N(\zeta_N = 20^\circ, \eta_N = 0^\circ)$ in the direction of the sun $\Omega_0(\zeta_0 = 32^\circ, \eta_0 = 0^\circ)$. The layer thickness is $z_t = 1$ m.

we define an index of the effect P_{index}, that is, the weighted sum of the BRF relative difference for each direction, given by

$$P_{index} = \sqrt{\frac{1}{M} \sum_{\underline{\Omega}_V} (\rho(\zeta_N, \underline{\Omega}_V)^2 \cdot \cos\zeta_V)} \qquad (15)$$

where $\cos\zeta_V$ represents the weighting for each direction, and M is the number of directions. This weighting was chosen because in most of the cases, a satellite-borne radiometer cannot observe with a zenith angle greater than 70°. In this way, we emphasize the relative difference in the BRF around nadir, which is particularly important from the point of view of remote sensing of the earth's surface. We computed this index for red and NIR wavelengths and for all LAD types. Hereafter, we call this index the "VVM index." We used four optical depths of the canopy: 1, 2, 5 and 10 m, respectively, and four different slope orientations, consisting of two slope angles of 10° and 20°, each pointing both toward and away from the sun direction.

Fig. 9 shows the VVM index at red and NIR wavelengths for both a 20° [Fig. 9(a)] and 10° [Fig. 9(b)] slope. In these figures, we represent the values with and without the hot spot correction with the same symbols. The values with the hot spot correction are always slightly higher than those without the hot spot correction.

When the LAD and the optical depth of the canopy are fixed, the VVM index is smaller for a 10° slope than for a 20° slope by a factor larger than 1.5 for both red and NIR wavelengths. The effect of the terrain slope therefore decreases with decreasing slope angle, as expected. For a given sun/terrain-slope configuration, the VVM index varies with the optical depth of the canopy, the wavelength, and the type of LAD. The VVM index is, in general, larger for red than for NIR wavelengths for all

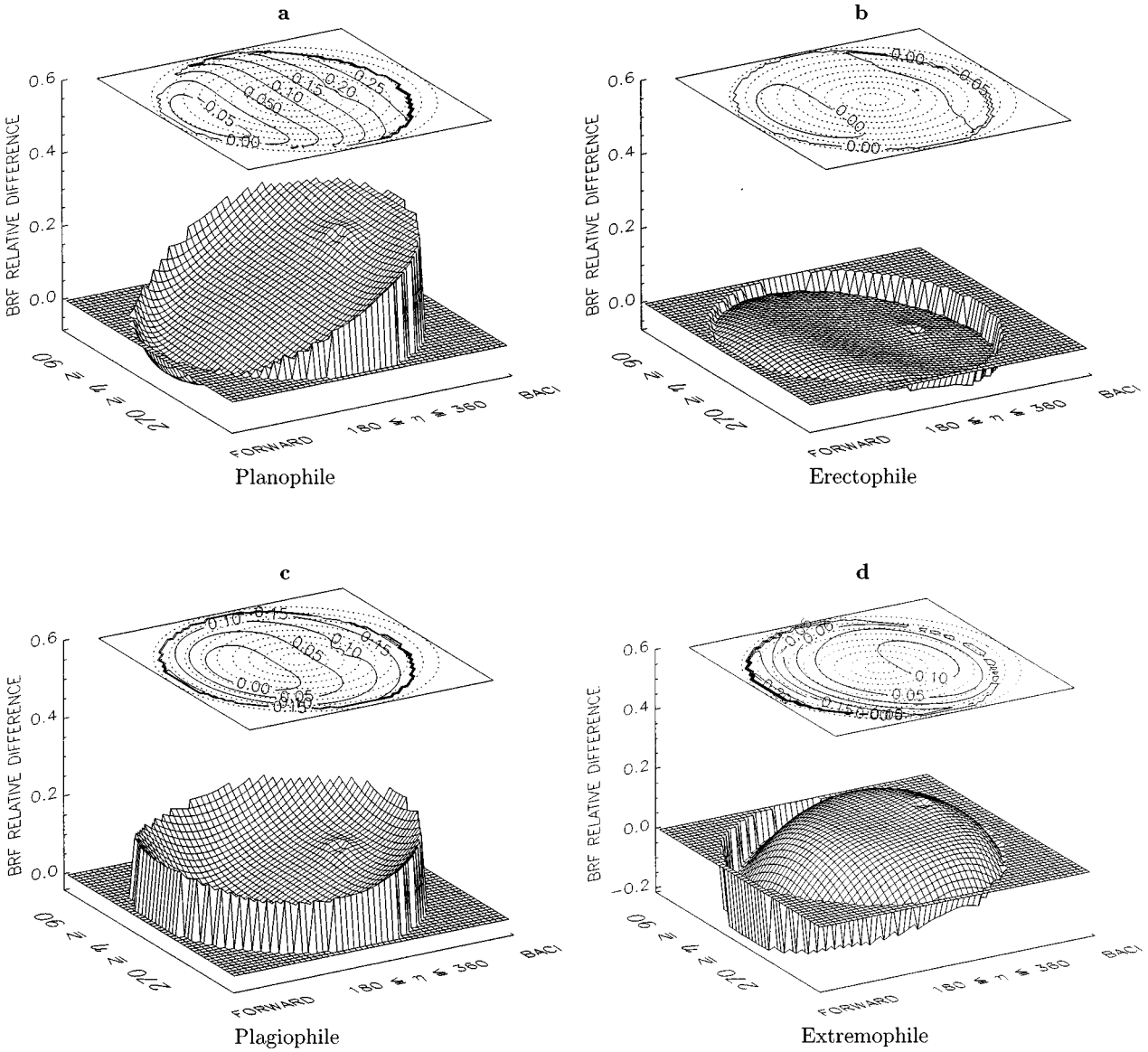

Fig. 8. BRF relative difference between the VVM and PGVM for red wavelengths. The terrain has a slope $N(\zeta_N = 20°, \eta_N = 180°)$ in the opposite direction to the sun $\Omega_0(\zeta_0 = 32°, \eta_0 = 0°)$. The layer thickness is z_t = 1 m.

types of LAD except extremophile. However, the index exhibits a larger variation with optical depth for NIR than for red wavelengths, again, except for the extremophile. Another interesting point is that the VVM index for NIR wavelengths decreases as the optical depth of the canopy increases, whereas its counterpart at red wavelengths exhibits only a very slight dependence on optical depth for all LAD types except the extremophile. As expected, the planophile LAD shows the largest VVM index at both red and NIR wavelengths for most of the situations modeled except for red wavelengths, for which the terrain is tilted toward the sun. In this latter situation, the VVM index becomes larger for the extremophile than for the planophile canopy. The erectophile LAD is the least sensitive to the effect of plant stand orientation. These results tend to show that the extremophile behaves in quite a different manner from the other LAD types.

4) Comparison with Measured Data: A preliminary validation of the VVM approach has been performed using reflectance data derived from measurements of radiance from a canopy of juvenile trees placed on a topographically orientable platform. The experimental system, described in detail elsewhere [25], allows the slope and azimuth of the canopy to be varied independently as a function of sun zenith and azimuth angles. A simple imaging radiometer, constructed from a digital camera and a filter wheel, is used to measure variations in radiance. Using this system, a set of radiance data has recently been acquired for a broad-leaved canopy (*pittosporum tenuifolium* var. silver sheen). Measurements were made as a function of sun azimuth and view zenith angles for the canopy when horizontal and at a 45° slope. The sun zenith angle was 32° and varied less than ±2° during measurements. The broad-leaved *pittosporum* canopy can be considered as having an approximately planophile LAD, which is the canopy type that exhibits the largest BRF relative differences in Figs. 7–9.

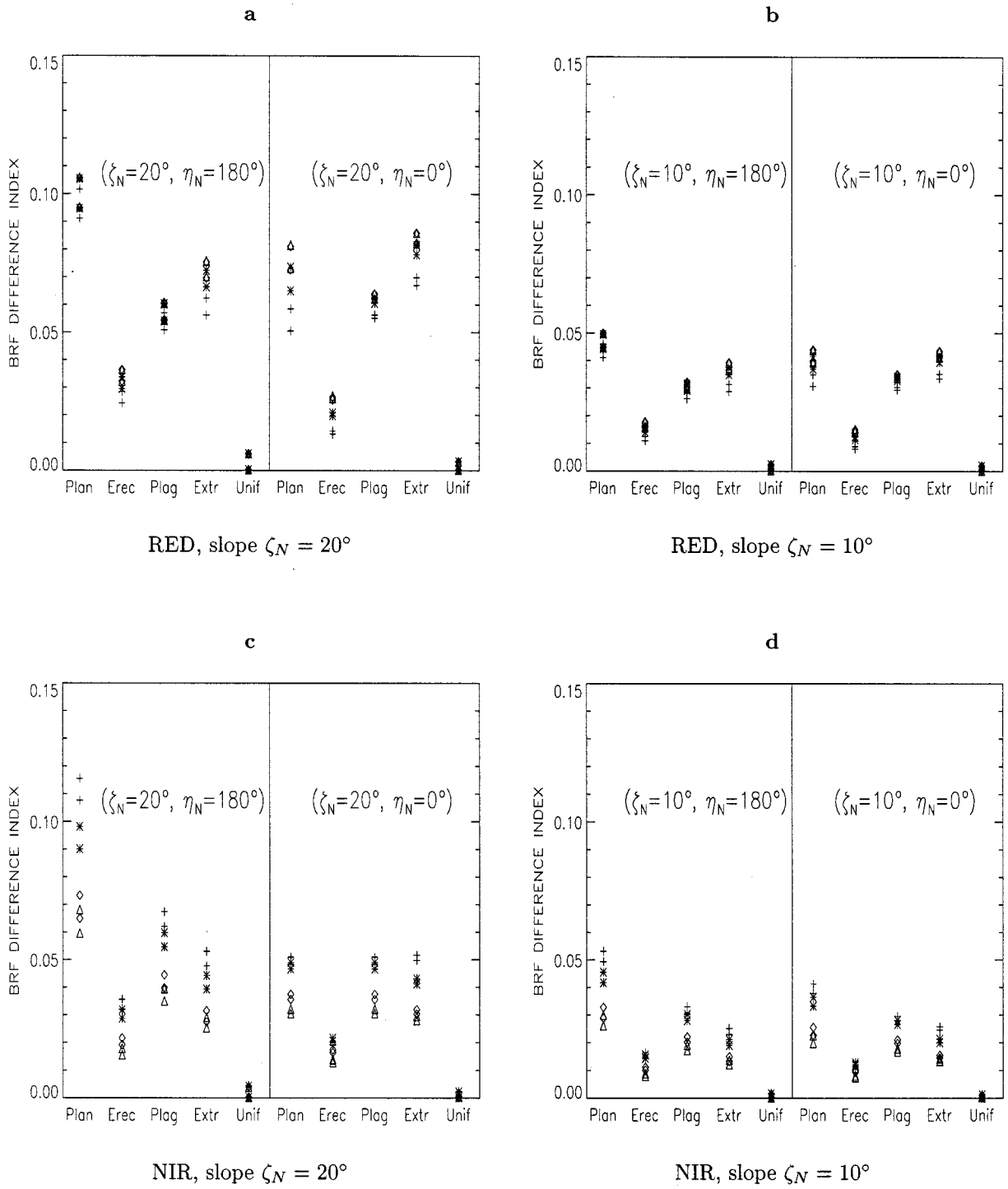

Fig. 9. VVM index for red and NIR wavelengths for slopes of ζ_N =20° and $\zeta_N = 10°$. For each case, the slope is oriented with $\eta_N = 180°$ (away from the sun) or $\eta_N = 0°$ (toward the sun). Leaf orientations are: planophile (plan), erectophile (erec), plagiophile (plag), extremophile (extr), and uniform (uni). The VVM index is calculated for $z_t = 1$ (+), 2 (∗), 5 (◇), and 10 m (△), with and without the hot spot. The index value is always larger if the hot spot is included.

To compare the VVM results with the experimental data, we make use of the parameter $BRF(\zeta_N = 45°)/BRF(\zeta_N = 0°)$, the ratio of canopy reflectance at a slope angle of 45° to that when the canopy is horizontal. The variation in this parameter as predicted by the VVM as a function of view zenith and sun azimuth angles is quite large and is shown in Fig. 10. Experimental data, available for a subset of the conditions shown in Fig. 10, are given in Table III, together with values predicted by both the VVM and PGVM approaches. In the case of the VVM, the agreement between the measured and predicted values of the reflectance ratio is most encouraging, with values usually agreeing within the expected measurement error. Considerably poorer agreement is obtained between measured reflectance ratios and those predicted with the PGVM, particularly at larger

TABLE III

COMPARISON OF MEASURED REFLECTANCE RATIOS FOR A BROAD-LEAVED CANOPY WITH THOSE PREDICTED FROM THE VVM AND PGVM FOR A PLANOPHILE CANOPY, AT A SLOPE ANGLE OF 45°. THE ACCURACY OF THE MEASURED REFLECTANCE RATIOS IS ESTIMATED AS ±10%. NEGATIVE VIEW ZENITH ANGLES INDICATE AN OFF-NADIR ANGLE IN THE DIRECTION OF THE TOP OF THE SLOPE. SLOPE AZIMUTH ANGLES ARE MEASURED RELATIVE TO THE PRINCIPAL PLANE

Wavelength	Slope azimuth angle (°)	View zenith angle (°)	$\frac{BRF(\zeta_N=45°)}{BRF(\zeta_N=0°)}$ Measured	Predicted with VVM	Predicted with PGVM
RED	0	+45	0.80	0.78	0.78
		0	1.11	1.10	1.14
		−30	1.28	1.40	1.23
	90	+45	0.87	0.94	0.98
		0	1.31	1.45	0.94
		−30	1.75	2.03	0.96
	180	+45	1.21	1.17	0.96
		0	2.04	1.92	0.98
		−30	3.43	3.26	0.73
NIR	0	+45	0.94	0.93	0.96
		0	1.17	1.12	1.08
		−30	1.22	1.28	1.12
	90	+45	1.00	1.11	0.99
		0	1.27	1.39	0.97
		−30	1.54	1.73	0.99
	180	−45	1.27	1.27	1.07
		0	1.73	1.66	1.05
		−30	2.35	2.67	0.88

slope azimuth angles and as view zenith angles decrease. It should be noted that the reflectance ratios derived from radiance measurements have been corrected for the effects of diffuse illumination, because the reflectance ratio predicted by the VVM or PGVM is that for direct beam illumination only. This correction has been performed by assuming that the diffuse irradiance is uniformly distributed over the sky hemisphere and has a magnitude such that 10% of the radiance from a horizontal canopy is from diffuse sources.

IV. CONCLUSIONS

A 1-D model was developed for bidirectional reflectance from a plant canopy on a hillslope. The model takes account of both the terrain slope and the tendency of plants to grow vertically regardless of slope because of the orienting effects of gravity. The model is based on the turbid medium assumption and includes a correction for the hot spot effect. This model, the VVM, was compared with a classical PGVM to evaluate the impact of plant stand orientation and terrain slope on the albedo and BRF of a vegetation canopy for a range of leaf angle distributions.

The albedo of a vegetation canopy on tilted terrain may become larger or smaller than that of horizontal terrain for both the VVM and PGVM, depending on the particular configuration of the sun direction and terrain slope. In addition to the effect of terrain slope, the albedo of the vegetation canopy also shows a dependence on the orientation of the plant stand. The relative difference in the albedo calculated using the VVM and PGVM approaches is less than 10% for small to moderate slope angles and reaches 20% when illuminated at very oblique incidence angles. The amplitude and sign of the albedo relative difference changes significantly with the type of leaf orientation, with the largest effects being observed for a planophile LAD and the smallest for an erectophile LAD.

The effect of plant stand orientation on the BRF follows no simple general rule in terms of variation with the optical depth of the canopy, sun/terrain-slope configuration, wavelength, or LAD type. The relative difference in the BRF's calculated using

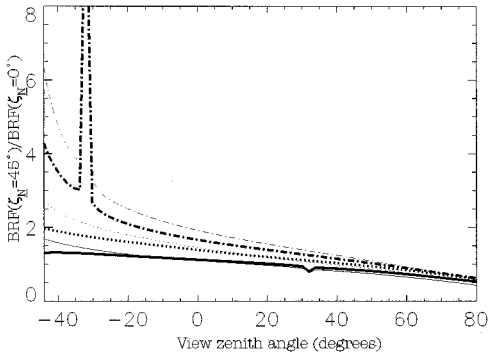

Fig. 10. Ratio of $BRF(\zeta_N = 45°)/BRF(\zeta_N = 0°)$ as modeled with the VVM for red (thin lines) and NIR (thick lines) wavelengths at a sun zenith angle of 32° and slope azimuth angles relative to the principal plane of 0° (continuous line), 90° (dotted line), and 180° (dash and dot line).

the VVM and PGVM changes greatly in overall pattern, amplitude, and sign with LAD type and sun/terrain-slope configuration. For the planophile, plagiophile, and extremophile LAD's, the relative difference can reach more than $\pm 10\%$ for small to moderate observation angles of less than 60° off-nadir.

The retrieval of earth surface characteristics relies on the measurement of radiance in the range of observation angles up to 60°. This means that both terrain slope and plant stand orientation must be taken into account for accurate retrieval of earth surface vegetation parameters. The use of the PGVM assumption for parameter retrieval over sloped terrain may lead to significant errors in the values of the parameters because of the orienting effects of gravity on plant stands. Present indications, based on an initial comparison of predicted and measured reflectance ratios, suggest that predictions of the VVM are consistent with changes in reflectance observed for real vegetation canopies as a function of variation in terrain slope, wavelength, and view zenith and slope azimuth angles. Since the computing cost in using the VVM is not much greater than that of the PGVM, it may be more appropriate to use the VVM in the retrieval of earth surface vegetation parameters.

REFERENCES

[1] K. T. Kriebel, "Measured spectral bidirectionnal reflection properties of four vegetated surfaces," *Appl. Opt.*, vol. 17, no. 2, pp. 253–259, 1978.

[2] D. S. Kimes and P. J. Sellers, "Inferring hemispherical reflectance of four vegetated surfaces," *Remote Sensing Environ.*, vol. 18, pp. 205–223, 1985.

[3] D. W. Deering, E. M. Middleton, and T. F. Eck, "Reflectance anisotropy for a Spruce-Hemlock Forest Canopy," *Remote Sensing Environ.*, vol. 47, pp. 242–260, 1994.

[4] M. M. Verstraete, B. Pinty, and R. Dickinson, "A physical model of the bidirectional reflectance of vegetation canopies. 1. Theory," *J. Geophys. Res.*, vol. 95, no. D8, pp. 11 755–11 765, July 1990.

[5] T. Nilson and A. Kuusk, "A reflectance model for the homogeneous plant canopy and its inversion," *Remote Sensing Environ.*, vol. 27, pp. 157–167, Feb. 1989.

[6] J. L. Privette, R. B. Myneni, C. J. Tucker, and W. J. Emery, "Invertibility of a 1D discrete ordinates canopy reflectance model," *Remote Sensing Environ.*, vol. 48, pp. 89–105, 1994.

[7] C. Proy, D. Tanré, and P. Y. Deschamps, "Evaluation of topographic effects in remotely sensed data," *Remote Sensing Environ.*, vol. 30, pp. 21–32, 1989.

[8] K. I. Itten and P. Meyer, "Geometric and radiometric correction of TM data of mountanous forested areas," *IEEE Trans. Geosci. Remote Sensing*, vol. 31, pp. 764–770, July 1993.

[9] J. A. Smith, T. L. Lin, and K. J. Ranson, "The Lambertian assumption and Landsat data," *Photogramm. Eng. Remote Sensing*, vol. 46, pp. 1183–1189, Sept. 1980.

[10] C. B. Schaaf, X. Li, and A. H. Strahler, "Topographic effects on bidirectional and hemispherical reflectances calculated with a geometric-optical canopy model," *IEEE Trans. Geosci. Remote Sensing*, vol. 32, pp. 1186–1193, Nov. 1994.

[11] B. N. Holben and C. O. Justice, "The topographic effect on spectral response from Nadir-Pointing sensors," *Photogramm. Eng. Remote Sens.*, vol. 46, no. 9, pp. 1191–1200, Sept. 1980.

[12] C. O. Justice, S. W. Wharton, and B. N. Holben, "Application of digital terrain data to quantify and reduce the topographic effect on Landsat data," *Int. J. Remote Sens.*, vol. 2, no. 3, pp. 213–230, 1981.

[13] J. Ross, *The radiation regime and architecture of plant stands*, Dr. W. Junk, Ed. Boston, MA, 1981.

[14] S. Chandrasekhar, *Radiative Transfer*. New York: Dover, 1960.

[15] J. Iaquinta and B. Pinty, "Adaptation of a bidirectional reflectance model including the hot-spot to an optically thin canopy," in *Proc. 6th Int. Symp. Physical Measurements and Signatures in Remote Sensing*, Val d'Isère, Frane, Jan. 21, 1994, pp. 683–690.

[16] R. B. Myneni, V. P. Gutschick, G. Asrar, and E. T. Kanemasu, "Photon transport in vegetation canopies with anisotropic scattering. Part IV. Discrete-ordinates/exact/kernel technique for two-angle photon transport in slab geometry," *Agr. Forest Meteorol.*, vol. 42, pp. 101–120, 1988.

[17] B. Hapke, D. DiMucci, R. Nelson, and W. Smythe, "The cause of the hot spote in vegetation canopies and soils: Shadow-hiding versus coherent backscatter," *Remote Sensing Environ.*, vol. 58, pp. 63–68, 1996.

[18] J. K. Shultis and R. B. Myneni, "Radiative transfer in vegetation canopies with anisotropic scattering," *J. Quant. Spectrosc. Radiat. Transf.*, vol. 39, pp. 115–129, 1988.

[19] N. J. J. Bunnik, *The Multispectral Reflectance of Shortwave Radiation by Agricultural Crops in Relation with Their Morphological and Optical Properties*. Wageningen, The Netherlands: Pudox, 1978.

[20] N. Goel and D. E. Strebel, "Simple beta distribution representation of leaf orientation in vegetation canopies," *Agron. J.*, vol. 76, pp. 800–802, 1984.

[21] J. Ross and A. L. Marshak, "The influence of leaf orientation and the specular component of leaf reflectance on the canopy bidirectional reflectance," *Remote Sensing Environ.*, vol. 27, pp. 251–260, 1989.

[22] R. B. Myneni, A. L. Marshak, and Y. V. Knyazikhin, "Transport theory for a leaf canopy of finite-dimensional scattering centers," *J. Quant. Spectrosc. Radiat. Transf.*, vol. 46, no. 4, pp. 259–280, 1991.

[23] A. L. Marshak, "The effect of the hot spot on the transport equation in plant canopies," *J. Quant. Spectrosc. Radiat. Transf.*, vol. 42, no. 6, pp. 615–630, 1989.

[24] J. Iaquinta, "Champs de rayonnement emergeant des surfaces terrestres: Modélization et inversion dans le cas de milieux optiquement finis et couplés avec une couche atmosphérique," M. A.thesis, Univ. Blaise Pascal, Clermont-Ferrand, France, 1995.

[25] C. M. Trotter, "Characterising the topographic effect at red wavelengths using juvenile conifer canopies," *Int. J. Remote Sensing*, vol. 19, no. 11, pp. 2215–2221, 1998.

Bruno Combal received the Maîtrise de Physique degree in 1994 and the DEA in Sciences de la Terre et de l'Atmosphère degree in 1995, both from the Université Blaise Pascal, Clermont-Ferrand, France, where he is currently pusuing the Ph.D degree.

In 1996, he was with the Laboratoire d'Aérologie, Toulouse, France, where he modeled the disruption of raindrops in a horizontal electric field.

Harumi Isaka received the M.Sc. degree in geophysics from Tohoku University, Sendai, Japan, in 1961, and the Docteur d'tat degree in physics from the Universit de Clermont-Ferrand, Clermont-Ferrand, France, in 1969.

He was a Charg de Recherche and later a Directeur de Recherche of the Centre National de la Recherche Scientifique, Université de Clermont-Ferrand, from 1966 to 1991. Since 1992, he has been a Professor in the Dèpartement of Physics and the Director of the Laboratoire de Météorologie Physique, Université de Clermont-Ferrand II. His research interests include turbulence in the atmospheric boundary layers, heterogeneous nucleation theory, cloud physics, and cloud modeling. His current interests focus on the radiative transfer theory in inhomogeneous media, scattering characteristics of nonspherical particles, and inverse problems in the atmospheric physics.

Craig Trotter received the B. Sc. degree (Honors) in physical and theoretical chemistry and the Ph.D. degree in biophysics, both from Massey University, Palmerston North, New Zealand, in 1976 and 1980, respectively.

He is currently a Senior Research Scientist with Landcare Research, Palmerston North. He has held prior positions in several research agencies, initially working in the areas of soil physics and ground water hydrology, micrometeorology, and the integrated use of GIS and remote sensing for land use assessment. His primary research interests now include measuring and modeling BRDF effects with particular reference to topographic correction, the use of remote sensing in spatial and physiological modeling of forest carbon dynamics, and the application of high spectral resolution data to detection of forest diseases. He is also a Principal Investigator for the ADEOS-II GLI sensor and a Co-Investigator for RADARSAT.